SEMARAK ILMU PUBLISHING

Journal of Advanced Research in Applied Mechanics

Journal homepage:
https://semarakilmu.com.my/journals/index.php/appl_mech/index
ISSN: 2289-7895

Performance Evaluation of RC Structures using Next- Generation Performance-Based Seismic Assessment Procedures

Amey Raju Khedikar[1,*], Mohd. Zameeruddin[2], Prabhakar Charpe[1], Dheeraj Deshmukh[3], Sneha Hirekhan[4]

[1] Department of Civil Engineering, Kalinga University, Naya Raipur, Chhattisgarh, 400 019, India
[2] Department of Civil Engineering, MGM's College of Engineering, Nanded, Maharashtra, 431 605, India
[3] Mechanical Engineering Department, Tulsiramji Gaikwad Patil College of Engineering and Technology, Nagpur, Maharashtra, 441108, India
[4] Department of Civil Engineering, Yeshwantrao Chavan College of Engineering (YCCE), Nagpur 441110, Maharashtra, 431 605, India

ARTICLE INFO

Article history:
Received 21 August 2024
Received in revised form 23 September 2024
Accepted 30 September 2024
Available online 30 October 2024

Keywords:
Performance-based seismic evaluation; Performance-based seismic assessment; correlation of damage index; example MRF; damage indices; integrate structural damages

ABSTRACT

Seismic forces have wreaked havoc on buildings around the world, resulting in both property damage and human deaths. Reinforced concrete structures under cyclic loading cannot be predicted using current methods, according to relevant design codes. Code-based seismic design procedures have been replaced by performance-based design procedures (PBSD). PBSD describes a building's overall performance by taking into account its structural and non-structural performance categories. Immediate occupancy, life safety, and collapse prevention are the three types of damage that can be encountered in a construction site. They are ranked based on the amount of damage, downtime, and casualties they inflict. Although these procedures can detect damage, they are unable to assign a numerical value to the seriousness of the damage. The use of damage indices, which are based on structural and response-based parameters, has been proposed by many researchers in the past. The objective of current research is an attempt to summarise all of these efforts and identify grey areas for further investigation. Numerical approaches to integrate structural damages with various PBSD performance levels have been proposed.

1. Introduction

Structural engineers are now more concerned with ensuring structural safety in the event of a seismic event because of the lessons learned from previous earthquakes. The current practice in India and the subcontinent for designing reinforced concrete structures subjected to lateral loads is force-based [1]. The inelastic behaviour of structural components is clutched into consideration by applying acceptable risk limits to the strength of materials, design loads, and serviceability of structures. A more powerful earthquake, however, destroyed the structures, which had previously withstood damage from smaller quakes. [2]

* *Corresponding author.*
E-mail address: amey.khedikar@gmail.com

https://doi.org/10.37934/aram.126.1.3348

Predictive methods of design have become more common as earthquake engineering knowledge has grown. According to Ghosh and colleagues (2011), the most common practises under predictive methods of design are; capacity-based, energy, strength and stiffness-based approaches, displacement-based approaches and comprehensive design considering life cycle costs. When all of the aforementioned techniques are used, the process is referred to as "performance-based seismic design"(PBSD). Seismic enactment of buildings is a primary concern for PBSD, which is why it was created [3].

PBSD's primary concerns in its current form are PBSE and PBA, or performance-based seismic evaluation and assessment (PBSA). This technique is used to assess the performance of PBSE structures. When assessing a building's performance, both structural and non-structural damage are considered [4]. Operating Levels (OP), Immediate Occupancy (IO), Life Safety (LS), and the Collapse Prevention Range (CP) are all parts of this umbrella term (C). It is impossible to enumerate the destruction created by a structural system collapsing when subjected to seismic loads using performance levels such as those used by Structural Engineers Association of California (SEAOC) 2000, Federal Emergency Management Agency (FEMA) 440 2005, [5].

There have been many attempts in the past to use Engineering Demand Parameters (EDPs) to estimate how much damage a structure or its components can take (EDPs). When a structure is subjected to seismic hazards and then tested again, engineers can obtain EDPs such as stress, strain, displacement, or stiffness. Scaled numerically from 0% to 100%, these EDPs evaluated structural and response-based parameters. As a result of these studies, the method is known as the "PBSA" procedure [2,6]. For a complete understanding of how a structure performs in a design earthquake, many researchers have attempted to integrate PBSE and PBSA procedures [7,8]. PBSA and PBSD progress will be examined in this study to see where we are at in terms of current knowledge. The integration of PBSE and PBSA has also been considered, to estimate the structure's performance and damage when associated with the design seismic circumstance [9].

2. Performance-based Seismic Evaluation

Performance-based seismic design (PBSD) approach has proven to be a better as an alternative to the perspective design approach. PBSD documents such as ATC 40 (Applied Technological Council), FEMA 356, ASCE 41 (American Society of Civil Engineers), and FEMA 440 has provided various PBSE methodologies. These documents had provided various modelling and acceptance criteria for nonlinear modelling of reinforced concrete (RC) sections [5,10,11].

Nonlinear static analysis procedures in the PBSD documents make use of pushover analysis (POA). The POA streamlines the process of applying incremental lateral loads to the structure when a plastic collapse mechanism is reached. A lumped-plasticity approach to analysis results in plastic hinges being formed on structural components during POA. Nonlinear response spectra are depicted in Figure 1 using the PBSE procedure, which takes into account capacity, demand, and performance point [12].

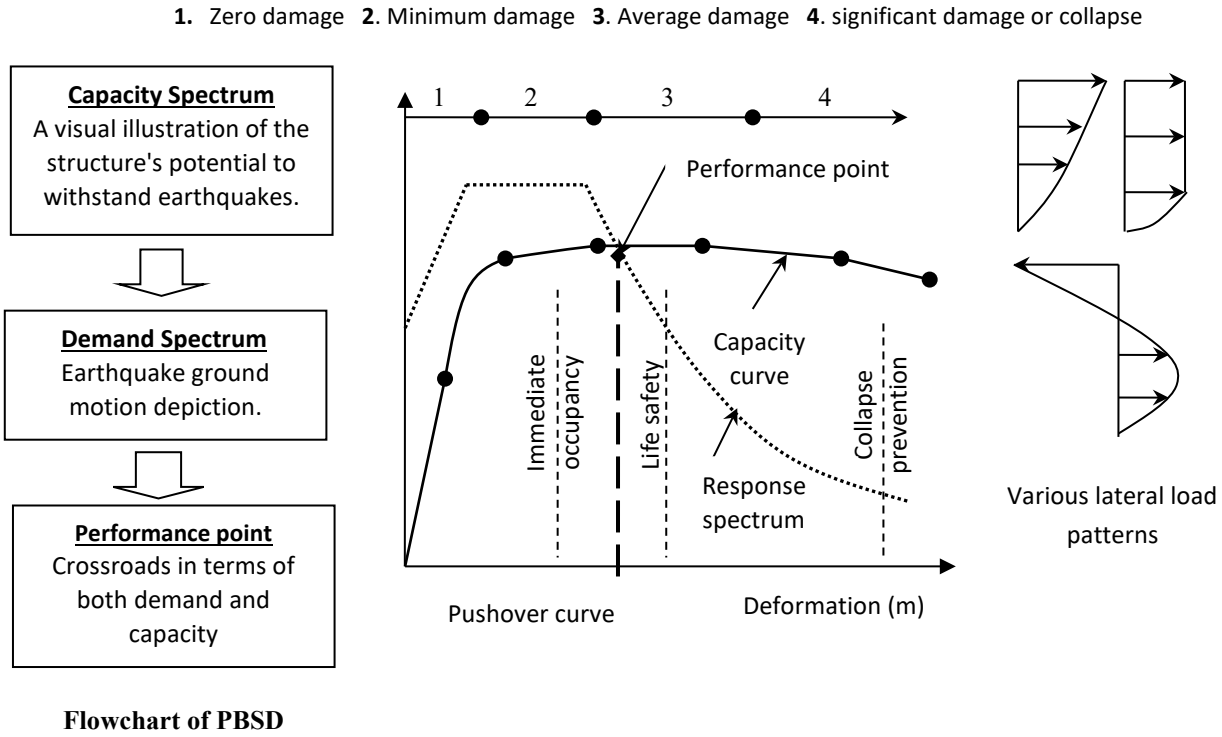

Fig. 1. Typical pushover analysis procedure

As its name suggests, this test is focused on determining how well a structure can withstand a seismic event. These performance limits have been established for both structural as well as non-structural components. The engineering demand parameters (EDPs) used to represent these performance stages can be found in [13]. Strain, stress, deformation, and damage to the member (including crack width) are all included in these EDPs. There are numerous PBSD performance objectives that were taken into consideration, as shown in Table 1.

Table 1
Performance levels with the associated damage states and drift limits

Conditions	Damage state	Drift
(IO) Immediately occupied, fully operational.	Zero Damage	< 0.2%
Operational, Damage under control, Average	Repairable	< 0.5%
Life safety: damage condition, close to collapse, limited safety	Irreparable	< 1.5%
Hazard reduced	critical	< 2.5%
Collapse	-	> 2.5%

Capacity Spectrum Method (CSM) and the Displacement Coefficient Approach are two alternatives in the PBSE method, which employs the nonlinear static method (NLSP) Displacement Coefficient Method (DCM). This includes [14], The structure's capacity or "capacity spectrum" is contrasted to the demand imposed on the structure in CSM (demand spectrum). It's the junction of these two curves that indicates the structure's reaction, which is the performance point. A diagram of the CSM method is shown in Figure 2(a). In DCM, the goal displacement is estimated by the application of coefficients. As seen in Figure 1, "target displacement" cites to the movement of a prominent node point, such as the roof of a structural system [15]. The DCM technique is shown in Figure 2(b). Improved methods for CSM and DCM were found in FEMA 440 and ASCE 41, the next generation of PBSD papers [8] demonstrate, these methods are thoroughly examined in their paper published in 2016.

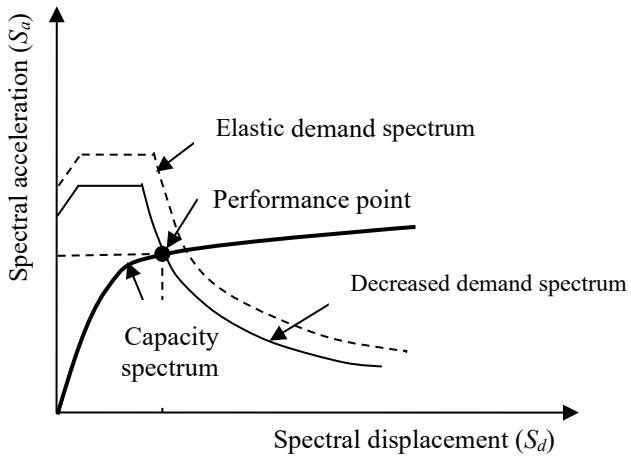

(a)

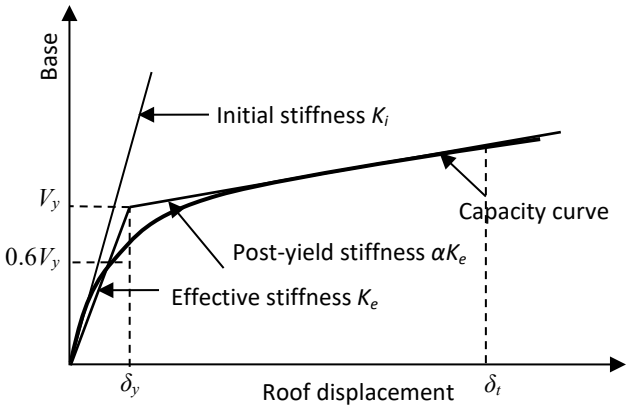

(b)

Fig. 2. (a) Capacity spectrum method (CSM) as per ATC 40 (b) Displacement coefficient method as per FEMA 273

3. Performance-based Seismic Assessment

To evaluate the behaviour of example, structure a damage index (DI) is needed to be defined [16]. The DI scales the damage state of a structure and its component parts in a numeric value which ranges from 0 to 1. When the value is "0," the state is undamaged, and when it is "1," the state is collapsed. It is possible to divide the DIs into two types: global and local. Locally produced documentaries the damage of individual members whereas global DI gives the weighted average of damages to all local DI at different structural levels. Based on the EDPs used in formulation of DI, DIs is further classified as response-based DI and structural parameter-based DI. These DI may be cumulative DI, Non-cumulative DI and Combined DI [17,18]. A comprehensive review of all DI's and their suitability are discussed in the literature by Zameeruddin and Sangle [19].

In elastic deformations cause damage in RC structures. Including deformation as a variable is why a DI exists. EDPs for global DI include the displacement of floors and the displacement between floors. Local DI is defined by the strain, cross-sectional curvature, and rotations at the member ends of a member. An RC member's degree of damage can be determined using figure 3 [8]. Nonlinear dynamic and static analysis results used by many research scholars in the past to define DIs. Nonlinear dynamic processes were uncommon in practise due to the complexities of the analysis process. However, addressing the cumulative effects of nonlinear static procedures is still under investigation [5,20].

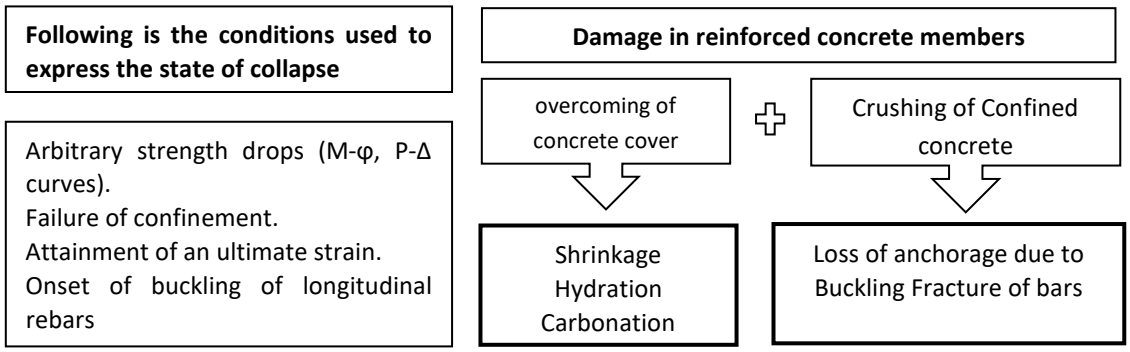

Fig. 3. Assessment of Damage Indices for RC Structures Based on PBSE and EDPs

Determination of the degree of impairment to RC members in its ongoing era PBSE procedures are able to predict the plastic-yield methodology of RC structures subjected to lateral loads, but they themselves are incapable to provide a damage value. This study aims to put forth some DIs using the EDPs obtained as a result of PBSE performed on RC structures.

4. Nonlinear Static Analysis

In order to attain the desired displacement value, it is essential to progressively raise the lateral loads in POA. The lateral loads on the RC structures replicate the inertia loads caused by a seismic event. Over the years, numerous scholars have presented a broad variety of lateral distribution patterns. since the lateral force profile impacts the structural behaviour, it is advised that a set of lateral load patterns be used while doing pushover analysis [21]. Ghobarah [2], should establish limits on inertia loads at the higher and lower end. In Stage I, the dispersed element loads were calculated from the yield line theory utilising gravity loads. Additionally, supplementary loads are taken into consideration in Stage I. It was necessary to remember the structure's condition once stage I was completed in order to apply the full loads (force-control). lateral loads were applied in a gradual manner in Stage II Push Over Analysis. A moment–rotation curve for an industry-standard plastic hinge was developed using FEMA 356-integrated software stress–strain relationships [22]. In order to mimic non-linear frame parts, such as beams and columns, plastic hinges were attached to both end portion of each beam or column. "Instant occupancy," "life-safety," and "collapse prevention" are labelled "immediate occupancy" and "life-safety" respectively in Figure 4.

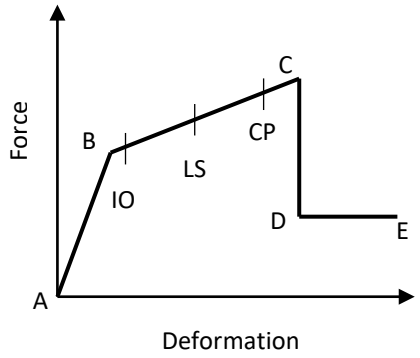

Acceptance criteria

	M/M_y	Rotation/ SF		Plastic deformation /SF	
A	0	0	0	3E-03	0.01
B	1	0	0	3E-03	0.01
C	1.1	0.015	0.025	0.012	0.02
D	0.20	0.015	0.025	0.015	0.025
E	0.20	0.015	0.05	0.015	0.025

Fig. 4. Relationship showing Force–deformation curve of a typical plastic hinge

5. Proposed Damage Indices

The nonlinear responses received as the product of POA performed on the example MRF were used to define the damage value. For assessing the performance of example MRF two performance level indicators are set as PL1 and PL2. PL1 includes the global responses corresponding to the performance levels OP, IO and LS. In PL2 responses at the performance levels CP, C, D and point E were used. The global EDPs considered in the study include storey displacement, base shear, and stiffness at various performance levels. The proposed damage indicators are drift-based, strength-based, and stiffness-based. This damage assessment is an attempt to extend the methodology proposed by Zameeruddin and Sangle [19] for the identification of damage zone using POA and PBSE methods.

6. Drift-based damage indicator (DI_d)

In PBSD different performance (criteria's) levels are defined on the basis of drift (conditions) limits as described in Table 1. With this limit's identification of performance levels and collapse mechanism is possible, but they do not provide any damage value. To overcome this limitation, drift-based damage index has been proposed. In DI_d the damage value is obtained using the available ductility at a considered performance level as described in Eq. (1).

$$DI_d = \frac{d_j - d_{OP}}{d_U - d_{OP}} \tag{1}$$

d_j, d_{op} and d_u are the storey displacement values at considered performance level, operational level, and permissible displacement at collapse (that is, 2.5 % H).

The POA's cyclic loading effects are attempted to be accounted for in this new formulation. Figure 5 demonstrates how the pushover curve is utilised to get the nonlinear responses needed for damage assessment.

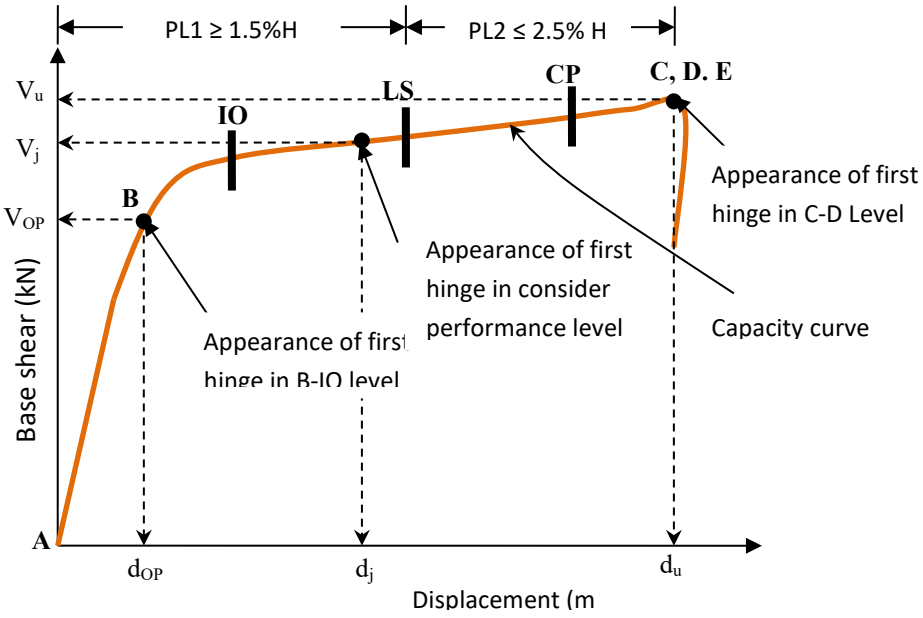

Fig. 5. Identification of nonlinear responses from capacity curve for DI calculation

7. Strength-based damage indicator (DI_s)

Base shear is used as a damage variable in strength-based DIs to reflect a reduction of strength during a POA. With the strength-based DI, structural behaviour during an inelastic displacement excursion may be accurately identified, leading to an objective way of evaluating the extent of the damage to a structure. The formula for the strength-based DIs is given in Eq. (2):

$$DI_S = \frac{V_j - V_{OP}}{V_{max} - V_{OP}} \tag{2}$$

where *V, V_{op} and Vmax* are the base shear values at considered performance level, operational level, and maximum base shear observed in POA.

8. Stiffness-based damage indicator (DI_k)

According to the suggested damage indicator, the damage value is evaluated by equating stiffness of the structure at any specified performance level to its operational stiffness. The stiffness-based DI is described in Eq. (3).

$$DI_k = 1 - \frac{K_j}{K_{OP}} \tag{3}$$

where; K_j, and K_{op} are the stiffness values at considered performance level and operational level. Many more EDPs may be used to evaluate damage value, as a preliminary attempt few of them are discussed herewith and others are kept as a scope for the future work.

9. Example MRF

MRFs that represent medium-rise buildings were tested for their response and damage states. The MRF as an example has three and four stories the example MRF underwent a displacement-controlled nonlinear static analysis (POA). Earliest, second, and third generation documents were used to analyse an example MRF's answer. SAP 2000 V 20.0 was used to model the sample structures analytically.

The example MRF has a 3-meter-wide bay and 3-meter-tall storeys. IS 456:2000, IS 1893:2002 (part 1), and IS 13920:1996 were used to design the example MRF. Lateral loads were applied to the frame, as shown in Figure 6. As an example, the MRF is situated in the seismic region V (z = 0.36) and importance constituent 1 (soil type). Table 2 lists the various material properties used to design structural members. Figure 6 depicts the example MRF's top view and front view. The details of RC section reinforcement are shown in table 3.

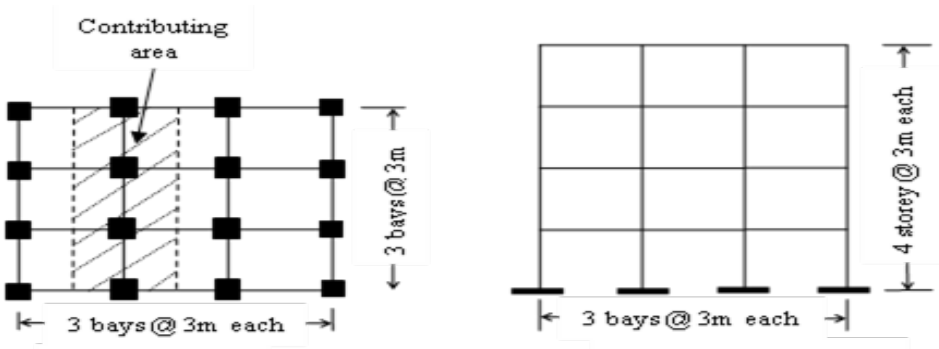

Fig. 6. Considered example of Moment Resistant Frame plan and elevation

Table 2
Summary of column size for Considered example of MRF

Storey	Outer column		Inner Column	
	dimension (mm)	Rebar's (mm^2)	dimension (mm)	Rebar's (mm^2)
All	380 x 380	6-20 mm φ	450 x 450	6-20 mm φ

Table 3
Summary of beam section for Considered example of MRF

Storey	Size (mm)	Rebar's (mm^2)								
		Bay 1			Bay 2			Bay 3		
		Top	Bot.	Top	Top	Bot.	Top	Top	Bot.	Top
1st	300 ×300	753	278	815	821	278	821	815	278	753
2nd		797	278	824	859	278	859	824	278	797
3rd		652	278	651	701	278	701	651	278	652
4th		390	345	518	532	314	532	518	345	390

Figure 7, shows the pushover curve of example MRF subjected to various lateral load patterns. All three lateral load patterns are used in POA; the earliest mode, the uniform load distribution, and the lateral load pattern obtained as per IS 1893. POA uses a variety of lateral load patterns, as shown in Figure 8.

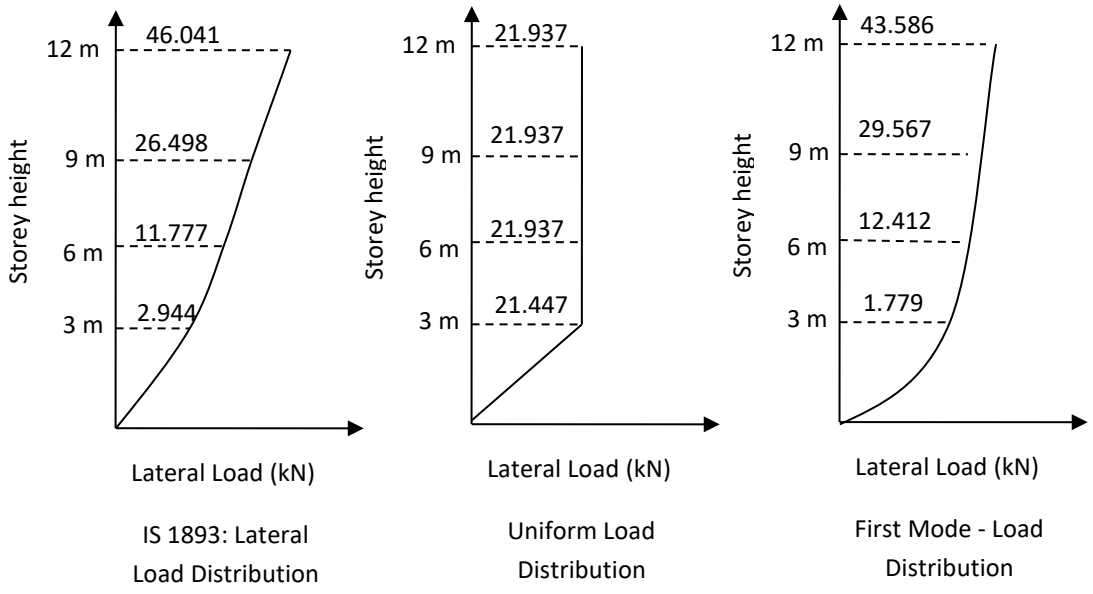

Fig. 7. Different lateral load patterns used in POA of example MRF

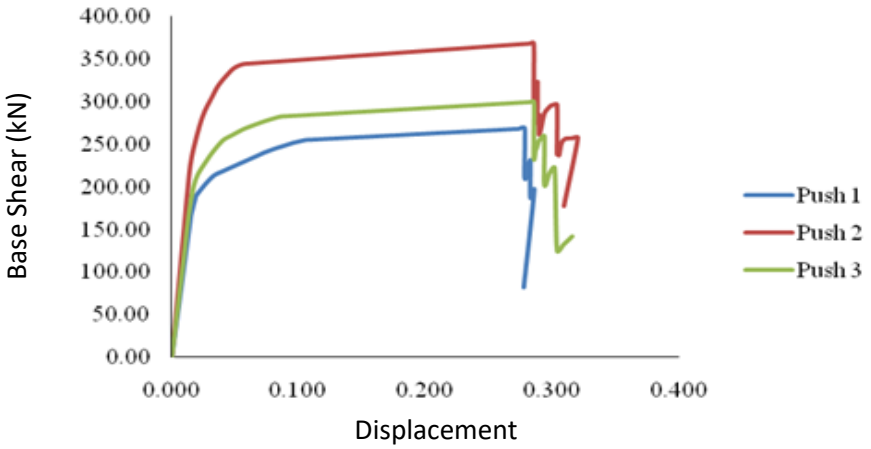

Fig. 8. Base shear-top displacement curve (Pushover curve) of example MRF subjected to various lateral loading cases

Table 4, table 5 and table 6 provides the collapse mechanism of example MRF under various lateral load patterns. Table 7 gives the nonlinear responses obtained, for example MRF in reference to various PBSE methods. Figure 9 represents the formation of plastic hinge mechanism at the collapse for different lateral load cases and its storey displacement shown in Figure 10.

From the nonlinear responses obtained from PBSE methods it is clear that, the behaviour of the structure under Push 1 and Push 3 load case is ductile, while the Push 2 load cases has yielded brittle failure mode of RC members which can be traced through the plastic hinge mechanism at collapse state. Nearly 10 percent of loss in the drift value has been observed in Push 2 load cases compared to Push 1 and Push 3 load cases. It may be concluded that the damages at middle storey levels are more in Push 2 load case as compared to other push load cases, hence to obtain a nonlinear response different lateral load patterns are needed to be applied.

Table 4
Collapse systems of Example MRF subjected to Push 1 Load case

Step No	Displ. (m)	Base shear (kN)	A To B	B to IO	IO to LS	LS to CP	CP to C	C to D	D to E	Beyond E	Total	Remarks
3	0.014	159.66	56	0	0	0	0	0	0	0	56	Operational Level
4	0.015	167.17	51	5	0	0	0	0	0	0	56	Actualization of earliest hinge in B-IO Performance Level
22	0.101	253.34	29	26	1	0	0	0	0	0	56	Actualization of earliest hinge in IO-LS Performance Level
59	0.278	268.40	28	0	27	0	0	1	0	0	56	Actualization of earliest hinge in C-D Performance Level
60	0.278	210.25	28	0	25	0	0	0	3	0	56	Actualization of earliest hinge in D-E Performance Level

Table 5
Collapse systems of Example MRF subjected to Push 2 Load case

Step No	Displ. (m)	Base Shear (kN)	A to B	B to IO	IO to LS	LS to CP	CP to C	C to D	D to E	Beyond E	Total	Remarks
2	0.010	151.52	56	0	0	0	0	0	0	0	56	Operational Level
3	0.013	198.88	55	1	0	0	0	0	0	0	56	Actualization of earliest hinge in B-IO Performance Level
21	0.105	349.81	28	26	2	0	0	0	0	0	56	Actualization of earliest hinge in IO-LS Performance Level
47	0.286	368.93	28	0	25	0	0	3	0	0	56	Actualization of earliest hinge in C-D Performance Level
48	0.286	304.61	28	0	25	0	0	0	3	0	56	Actualization of earliest hinge in D-E Performance Level

Table 6
Collapse systems of Example MRF subjected to Push 3 Load case

Step No	Disp. (m)	Base Shear (kN)	A to B	B to IO	IO to LS	LS to CP	CP to C	C to D	D to E	Beyond E	Total	Remarks
2	0.010	120.06	56	0	0	0	0	0	0	0	56	Operational Level
3	0.014	173.99	54	2	0	0	0	0	0	0	56	Actualization of earliest hinge in B-IO Performance Level
20	0.105	284.70	28	26	2	0	0	0	0	0	56	Actualization of earliest hinge in IO-LS Performance Level
55	0.286	300.22	28	0	26	0	0	2	0	0	56	Actualization of earliest hinge in C-D Performance Level
56	0.286	256.58	28	0	24	0	0	2	2	0	56	Actualization of earliest hinge in D-E Performance Level

Table 7
Nonlinear responses of example MRF in reference to various PBSE methods

Sr. No.	PBSE method	Push 1		Push 2		Push 2	
		BS Sh. (kN)	Displ. (m)	BS Sh. (kN)	Displ. (m)	BS Sh. (kN)	Displ. (m)
1	ATC 40 (CSM)	234.48	0.064	340.28	0.050	269.72	0.059
2	FEMA 440 (CSM)	241.61	0.075	344.86	0.058	276.96	0.072
3	FEMA 356 (DCM)	251.26	0.095	346.39	0.073	283.18	0.088
4	FEMA 440 (DCM)	256.52	0.125	347.56	0.084	286.02	0.109

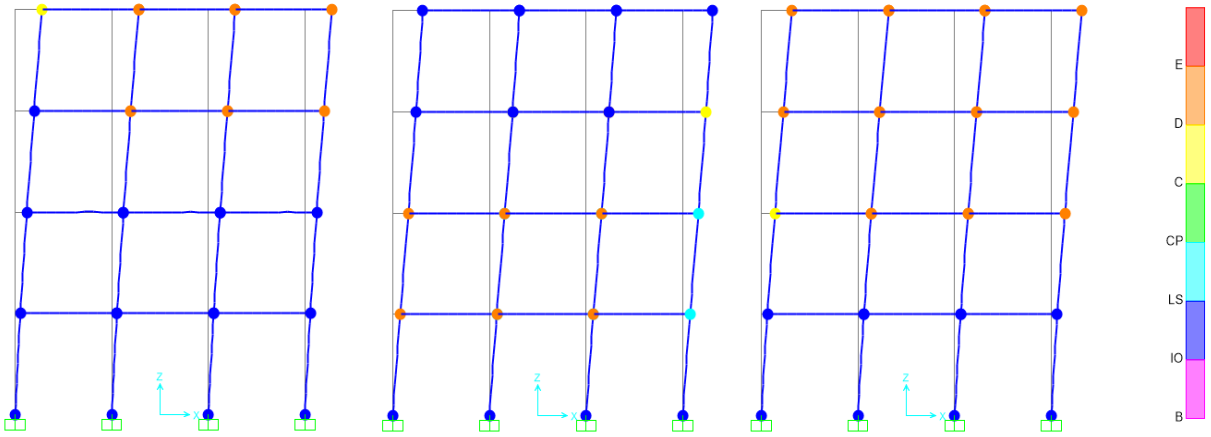

Collapse state for Push 1 Load Case | Collapse state for Push 2 Load Case | Collapse state for Push 3 Load Case

Fig. 9. Plastic hinge mechanism of example MRF at collapse state subjected to different lateral loads

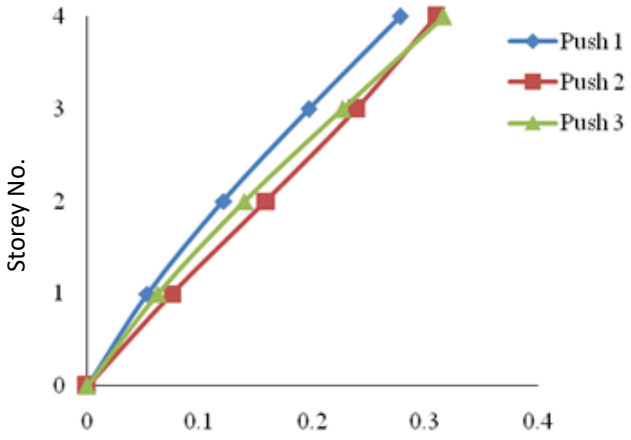

Fig. 10. Storey displacement of example frames under various lateral load cases

From Figure 11, it is observed that the rooftop displacement (inter storey drift) obtained in pushover 1 and pushover 3 load cases yield upper and lower bound values. Whereas; push 2 results in median values of displacement. Figure 9 also shows that the inter-storey drifts of middle stories are more in push 2 load case as compared to push 1 and push 3 load cases. The base shear, rooftop displacement and inter-storey displacement are the measure of global damage sustain by a structure, but do not yield any associated damage. This reflects the limitations of the available PBSE methods.

In this study attempt has been made to scale up the damage value by using the nonlinear response obtained from the results of PBSE methods. The displacement, base shear value at varied degrees of performance is used in the estimates of DI's. The fall of plastic hinges in respective performance levels are used as performance indicators. Two performance level indicators were used to identify the example MRF performance, subjected to different lateral load patterns namely, Performance Level-1 (PL1) and Performance Level-2 (PL2)

PL1 describes OP, IO, LS performance stages for which limits of drifts are referred as tabulated in Table 1 whereas; PL2 corresponds to CP, C, D and E performance levels. The actualization of plastic hinges in A-B level, the structure is assumed to be in OP. Successive fall of plastic hinge between to

B-C level are used for identifying the IO, LS and CP Level. Table 4, table 5, table 6 describes such identifications. The DI's represents the loss in drift value, strength, stiffness. Many more engineering parameters may be used for damage identification, but this study has been limited for predefined DI and keeps other DI's as a future scope of the study.

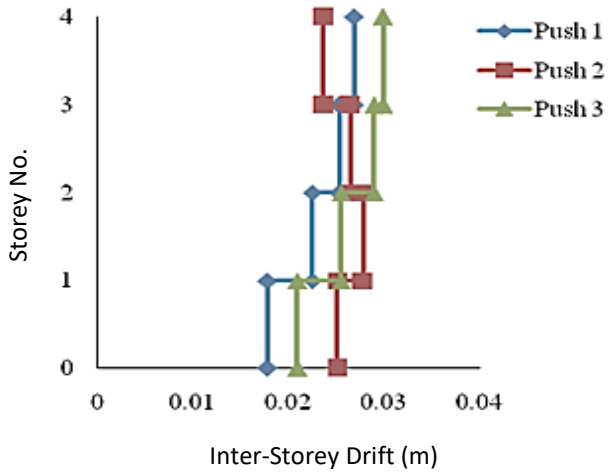

Fig. 11. Inter-storey drifts of frames under various lateral load cases

Figure 12 show the variation of DIs for various performance levels under different push load cases. From the observed values it may conclude that Pushover 1 and Pushover 2 load cases results top and bottom bound values of example MRF. Table 8, Table 9 and Table 10, provides the values of DI's obtained, for example MRFs using expression given in Eq. (1), Eq. (2) and Eq. (3). From the calculate values of DI_d, it may be concluded that the onset of damages for PL1 appears at lower values of drift compared to permissible limits (see Figure 13 and Table 9). Comparing to PL1 the damage values at PL2 appeared for drift values nearly equal to the permissible limits. The damage value at PL1 and PL2 obtained by linearization is 0.59 and 1.0. The reason for such behaviour may be attributed to the equilibrium between the compressive forces and tensile force of the RC sections which depends on the grade of steel. The identification of such zone helps to redesign the RC sections with improved ductility. The complete solution over such problems needs extensive research study on a bunch of example frames. The present study focuses on the identification of gray areas for improvements and complete solution is kept as scope for future work.

Table 8
Calculation of Drift-based DI value

Performance Level	Push 1				Push 2				Push 3			
	d_{op}	d_j	d_u	DI_d	d_{op}	d_j	d_u	DI_d	d_{op}	d_j	d_u	DI_d
OP	0.014	0.014	0.30	0.000	0.010	0.010	0.30	0.000	0.010	0.010	0.30	0.00
B-IO	0.014	0.015	0.30	0.002	0.010	0.013	0.30	0.010	0.010	0.014	0.30	0.015
IO-LS	0.014	0.101	0.30	0.302	0.010	0.105	0.30	0.328	0.010	0.105	0.30	0.330
C-D	0.014	0.278	0.30	0.924	0.010	0.286	0.30	0.951	0.010	0.286	0.30	0.951
D-E	0.014	0.278	0.30	0.924	0.010	0.286	0.30	0.951	0.010	0.286	0.30	0.951

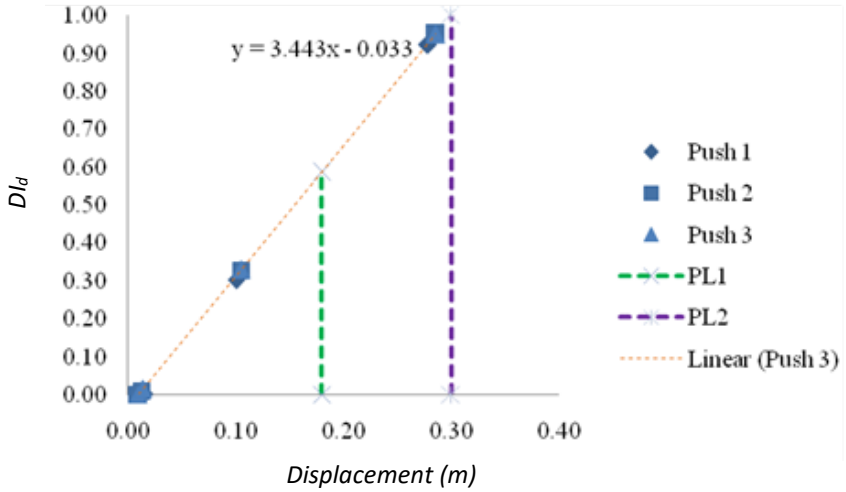

Fig. 12. Drift-based DI of example MRF for PL1 and PL2

Table 9
Calculation of Strength-based DI value

Performance Level	Push 1				Push 2				Push 3			
	V_{op}	V_j	V_{max}	DI_s	V_{op}	V_j	V_{max}	DI_s	V_{op}	V_j	V_{max}	DI_s
OP	159.6	159.6	268.4	0.000	151.5	151.5	368.9	0.000	120	120.06	300.2	0.00
B-IO	159.6	167.1	268.4	0.069	151.5	198.8	368.9	0.218	120	173.99	300.2	0.299
IO-LS	159.6	253.3	268.4	0.861	151.5	349.8	368.9	0.912	120	284.70	300.2	0.914
C-D	159.6	268.4	268.4	1.000	151.5	368.9	368.9	1.000	120	300.22	300.2	1.000
D-E	159.6	210.2	268.4	0.465	151.5	304.6	368.9	0.704	120	256.58	300.2	0.758

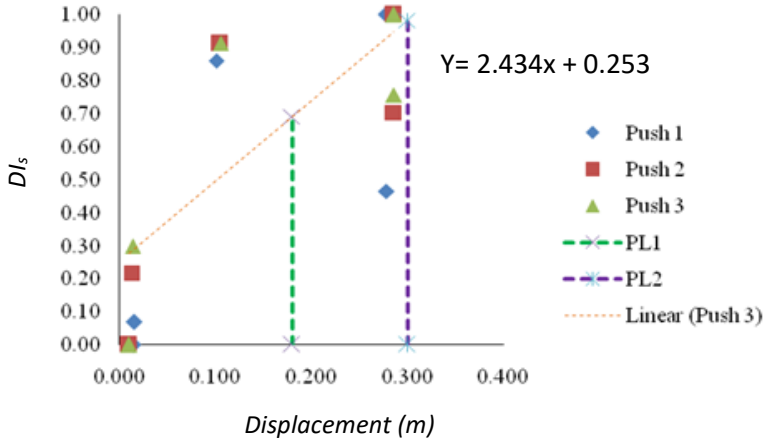

Fig. 13. Strength-based DI of example MRF for PL1 and PL2

With the incremental loading there is a fall in the stiffness of the structure (as shown in Figure 14), hence the available stiffness at a performance level can be used as a measure of damage. The damage value of a considered performance level is evaluated by measuring the stiffness of the joints at the operational state with the available stiffness at considered level.

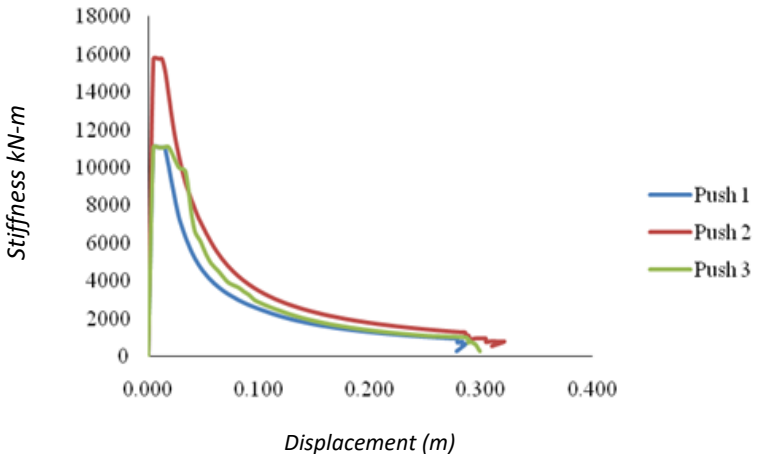

Fig. 14. Variation of stiffness of example under various push load cases

Table 10 provides the values DI_s obtained from nonlinear responses resulting from POA performed on example MRF. By linearization technique applied on results for Push 3 load case damage value obtained at PL1 and PL2 is 0.69 and 0.98. Table 10 and Figure 15 provide the values of DI_K obtained at various performance levels under different load cases. With the help of linearization DI_K at any value of displacement can be obtained. From the obtained relationship for push 3 load case the damage values at PL1 and PL2 are 0.65 and 1.0

Table 10
Calculation of Stiffness-based DI value

Performance	Push 1			Push 2			Push 2		
Level	K_{op}	K_j	DI_K	K_{op}	K_j	DI_K	K_{op}	K_j	DI_K
OP	11087.5	11087.5	0.000	15783.4	15783.4	0.000	12506.8	12506.8	0.00
B-IO	11087.5	11087.5	0.000	15783.4	15783.3	0.000	12506.8	12506.6	0.000
IO-LS	11087.5	2517.43	0.773	15783.4	3338.52	0.788	12506.8	2703.52	0.784
C-D	11087.5	964.79	0.913	15783.4	1291.54	0.918	12506.8	1050.12	0.916
D-E	11087.5	755.74	0.932	15783.4	1066.36	0.932	12506.8	897.43	0.928

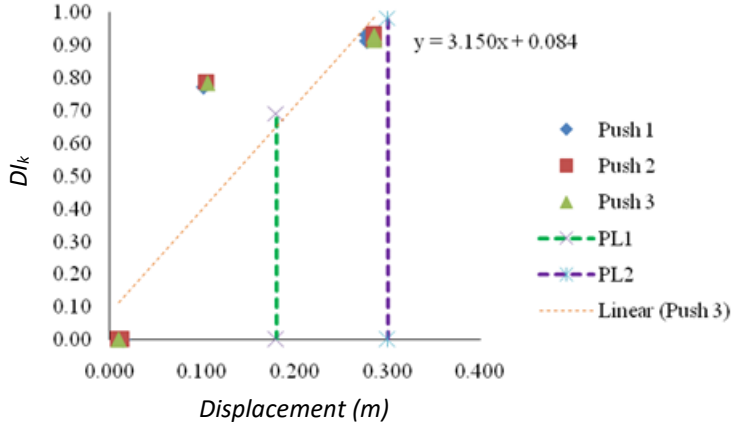

Fig. 15. Stiffness-based DI of example MRF for PL1 and PL2

10. Conclusions

Structural engineers are increasingly concerned about earthquake-related damage to buildings. Based on nonlinear dynamic analysis, the damage indicators in the literature can be used to assess

damage. This type of analysis is difficult and time-consuming, so it isn't common in the real world. PBSD has provided PBSE methods using NLSP for performance evaluation, but they are unable to provide a numerical value for the damage sustained by the structure and its components themselves. Here, we propose an approach for integrating the performance and damage parameters for a structure's damage assessment using the responses from POA Cyclic loads may be handled by this device. Di formulation has been evaluated at varying degrees of building performance to ascertain the current state of the art. The PBSE procedure has also been attempted to be integrated with damage values by defining DIs using EDPs resulting from POA.

The results of NLSP on an example MRF were used to determine a structure's damage value in relation to its performance. Two performance level indicators, PL1 and PL2, were devised to determine the extent of damage to the structure. Using a damage variable that accounts for the cumulative impacts of each incremental displacement can get over POA's constraint on evaluating a structure's ductility, strength loss, and stiffness loss. Damage may now be assessed at any point along the capacity curve owing to the DI's introductions. Performance levels PL1 and PL2 assist in determining where and how much structural design optimization can be done in the event of damage.

Acknowledgement
The authors declare that they have no known competing financial interests or personal relationships that could have appeared to influence the work reported in this paper. The said work has not been funded by any stakeholders in interest, it's purely academic research. There exists no conflict of interest from affiliated institutes or any other agencies.

References

[1] Hassoon, Alaa, and Khamail Abdul-Mahdi Mosheer. "Structural Behavior of Hybrid Reinforced Concrete Short Columns Under Uniaxial Load." *International Journal of Analytical, Experimental and Finite Element Analysis*, vol. 10, no. 1 (March 2023): 11-20. https://doi.org/10.26706/ijaefea.1.10.20239319

[2] Ghobarah, Ahmed. "Performance-based design in earthquake engineering: state of development." *Engineering structures* 23, no. 8 (2001): 878-884. https://doi.org/10.1016/S0141-0296(01)00036-0

[3] Boroujeni, Ali Reza Keyvani. "Evaluation of various methods of FEMA 356 compare to FEMA 440." *Journal of civil engineering and construction technology* 4, no. 2 (2013): 51-55. https://doi.org/10.5897/JCECT12.082.

[4] Quanjin, Ma, M. N. M. Merzuki, M. R. M. Rejab, M. S. M. Sani, and Bo Zhang. "Numerical investigation on free vibration analysis of kevlar/glass/epoxy resin hybrid composite laminates." *Malaysian Journal on Composites Science and Manufacturing* 9, no. 1 (2022): 11-21. https://doi.org/10.37934/mjcsm.9.1.1121

[5] Saleemuddin, Mohd Zameeruddin Mohd, and Keshav K. Sangle. "Seismic damage assessment of reinforced concrete structure using non-linear static analyses." *KSCE Journal of Civil Engineering* 21 (2017): 1319-1330. https://doi.org/10.1007/s12205-016-0541-2

[6] Mohammed, Waleed Khalid, and Khamees N. Abdulhaleem. "Finite Element Analysis of Self-Compacted Concrete Filled Steel Tube Columns Exposed to High Temperatures." *International Journal of Analytical, Experimental and Finite Element Analysis*, vol. 10, no. 1 (March 2023): 1-10. https://doi.org/10.26706/ijaefea.1.10.20239252

[7] Wang, Jer-Fu, Chi-Chang Lin, and Shih-Min Yen. "A story damage index of seismically-excited buildings based on modal frequency and mode shape." *Engineering Structures* 29, no. 9 (2007): 2143-2157. https://doi.org/10.1016/j.engstruct.2006.10.018.

[8] Zameeruddin, Mohd, and Keshav K. Sangle. "Review on Recent developments in the performance-based seismic design of reinforced concrete structures." In *Structures*, vol. 6, pp. 119-133. Elsevier, 2016. https://doi.org/10.1016/j.istruc.2016.03.001

[9] Hamzah, Khaldoon Hussein. "Heat Treatment After Sintering Process and Development of Porous Metal Materials." *International Journal of Analytical, Experimental and Finite Element Analysis*, vol. 10, no. 1 (March 2023): 21-28. https://doi.org/10.26706/ijaefea.1.10.20239556

[10] Priestley, M. J. N. "Displacement-based seismic assessment of reinforced concrete buildings." *Journal of earthquake engineering* 1, no. 01 (1997): 157-192. https://doi.org/10.1080/13632469708962365

[11] Xuan, Yeo Yi, Mohd Ridzuan Mohd Jamir, Mohd Shukry Abdul Majid, Mohd Shihabudin Ismail, Ferriawan Yudhanto, Normahira Mamat, and Fauziah Mat. "Cure Behaviour and Tensile Properties of Pineapple Leaf Fibre Reinforced Natural Rubber Composites." *Journal of Advanced Research in Applied Mechanics* 115, no. 1 (2024): 88-97. https://doi.org/10.37934/aram.115.1.8897

[12] Wang, Jer-Fu, Chi-Chang Lin, and Shih-Min Yen. "A story damage index of seismically-excited buildings based on modal frequency and mode shape." *Engineering Structures* 29, no. 9 (2007): 2143-2157. https://doi.org/10.1016/j.engstruct.2006.10.018.

[13] Ghosh, Siddhartha, Debarati Datta, and Abhinav A. Katakdhond. "Estimation of the Park–Ang damage index for planar multi-storey frames using equivalent single-degree systems." *Engineering Structures* 33, no. 9 (2011): 2509-2524. https://doi.org/10.1016/j.engstruct.2011.04.023

[14] Cardone, Donatello, and Giuseppe Gesualdi. "Seismic rehabilitation of existing reinforced concrete buildings with seismic isolation: a case study." *Earthquake Spectra* 30, no. 4 (2014): 1619-1642. https://doi.org/10.1193/110612EQS323M

[15] Talib, Mohd Khaidir Abu, Siti Nor Hidayah Arifin, Aziman Madun, Mohd Firdaus Md Dan, and Faizal Pakir. "Effect of Rice Husk Ash (RHA) as a Pozzolan on the Strength Improvement of Cement Stabilized Peat." *Journal of Advanced Research in Applied Mechanics* 114, no. 1 (2024): 83-93. https://doi.org/10.37934/aram.114.1.8393

[16] Deshmukh, Shital S. "Base Isolation: A Versatile Seismic Control Tool-A Review." *International Journal of Analytical Experimental and Finite Element Analysis (IJAEFEA)* 10 (3) (2023): 87–95. https://doi.org/10.26706/ijaefea.3.10.20230803

[17] Habibi, Alireza, Mahdi Izadpanah, and Azad Yazdani. "Inelastic damage analysis of RCMRFS using pushover method." *Iranian Journal of Science and Technology-Transactions of Civil Engineering* 37, no. c2 (2013). https://doi.org/10.22099/ijstc.2013.1623

[18] Wilson, E. L., and A. Habibullah. "SAP 2000/NL-push version 17 software, computer and structures." *Inc, Berkeley, CA, USA* (2000).

[19] Saleemuddin, Mohd Zameeruddin Mohd, and Keshav K. Sangle. "Seismic damage assessment of reinforced concrete structure using non-linear static analyses." *KSCE Journal of Civil Engineering* 21 (2017): 1319-1330.. https://doi.org/10.1007/s12205-016-0541-2

[20] Katman, Herda Yati Binti, Wong Jee Khai, Mehmet Serkan Kırgız, Moncef L. Nehdi, Omrane Benjeddou, Blessen Skariah Thomas, Styliani Papatzani, Kishor Rambhad, Manoj A. Kumbhalkar, and Arash Karimipour. "Transforming conventional construction binders and grouts into high-performance nanocarbon binders and grouts for today's constructions." *Buildings* 12, no. 7 (2022): 1041. https://doi.org/10.3390/buildings12071041

[21] Kırgız, Mehmet Serkan, André Gustavo de Sousa Galdino, John Kinuthia, Anwar Khitab, Muhammad Irfan Ul Hassan, Jamal Khatib, Hesham El Naggar et al. "Synthesis, physico-mechanical properties, material processing, and math models of novel superior materials doped flake of carbon and colloid flake of carbon." *Journal of Materials Research and Technology* 15 (2021): 4993-5009. https://doi.org/10.1016/j.jmrt.2021.10.089

[22] Iduwin, Tommy, Sigit Pranowo Hadiwardoyo, Andri Irfan Rifai, and Riana Herlina Lumingkewas. "Contribution of Plastic Waste in Recycles Concrete Aggregate Paving Block." *Journal of Advanced Research in Applied Mechanics* 110, no. 1 (2023): 1-10. https://doi.org/10.37934/aram.110.1.110